Corrections

MEDICAL SCIENCES

Correction for "Myc and mTOR converge on a common node in protein synthesis control that confers synthetic lethality in Myc-driven cancers," by Michael Pourdehnad, Morgan L. Truitt, Imran N. Siddiqi, Gregory S. Ducker, Kevan M. Shokat, and Davide Ruggero, which appeared in issue 29, July 16, 2013, of *Proc Natl Acad Sci USA* (110:11988–11993; first published June 26, 2013; 10.1073/pnas.1310230110).

The authors note that Fig. 5 appeared incorrectly. The corrected figure and its legend appear below.

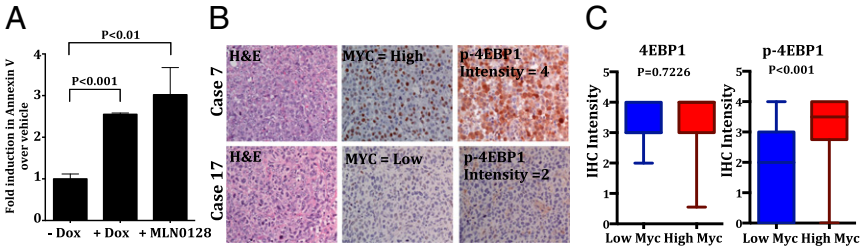

Fig. 5. Clinical relevance of mTOR-dependent 4EBP1 phosphorylation in Myc-driven human lymphomas. (*A*) Analysis of apoptosis in the human Raji Burkitt's lymphoma cell line upon $4EBP1^{m}$ expression or MLN0128 treatment for 24 h. Graph represents mean ± SD. (*B*) Representative H&E, Myc staining, and phospho-4EBP1 staining in human diffuse large B-cell lymphoma (DLBCL). (*C*) Box and whisker plot of IHC intensity for total 4EBP1 and phospho-4EBP1 from a human DLBCL tissue microarray (TMA) consisting of 77 patients.

www.pnas.org/cgi/doi/10.1073/pnas.1317701110

NEUROSCIENCE

Correction for "Identification of a μ-δ opioid receptor heteromer-biased agonist with antinociceptive activity," by Ivone Gomes, Wakako Fujita, Achla Gupta, Adrian S. Saldanha, Ana Negri, Christine E. Pinello, Edward Roberts, Marta Filizola, Peter Hodder, and Lakshmi A. Devi, which appeared in issue 29, July 16, 2013, of *Proc Natl Acad Sci USA* (110:12072–12077; first published July 1, 2013; 10.1073/pnas.1222044110).

The authors note that Christina Eberhart should be added to the author list between Christine E. Pinello and Edward Roberts. Christina Eberhart should be credited with having performed research and analyzed data.

The authors also note that the author name Adrian S. Saldanha should instead appear as S. Adrian Saldanha.

The corrected author line, affiliation line, and author contributions appear below. The online version has been corrected.

Ivone Gomes[a], Wakako Fujita[a], Achla Gupta[a], S. Adrian Saldanha[b], Ana Negri[c], Christine E. Pinello[b], Christina Eberhart[b], Edward Roberts[d], Marta Filizola[c], Peter Hodder[b], and Lakshmi A. Devi[a]

Departments of [a]Pharmacology and Systems Therapeutics and [c]Structural and Chemical Biology, Icahn School of Medicine at Mount Sinai, New York, NY 10029; [b]Scripps Research Institute Molecular Screening Center, Lead Identification Division, Translational Research Institute, Jupiter, FL 33458; and [d]Department of Chemistry, The Scripps Research Institute, La Jolla, CA 92037

Author contributions: P.H. and L.A.D. designed research; I.G., W.F., A.G., S.A.S., A.N., C.E.P., C.E., and E.R. performed research; E.R. and M.F. contributed new reagents/analytic tools; I.G., W.F., S.A.S., C.E.P., C.E., M.F., P.H., and L.A.D. analyzed data; and I.G. and L.A.D. wrote the paper.

www.pnas.org/cgi/doi/10.1073/pnas.1317238110

NEUROSCIENCE

Correction for "Transient, afferent input-dependent, postnatal niche for neural progenitor cells in the cochlear nucleus," by Stefan Volkenstein, Kazuo Oshima, Saku T. Sinkkonen, C. Eduardo Corrales, Sam P. Most, Renjie Chai, Taha A. Jan, Alan G. Cheng, and Stefan Heller, which appeared in issue 35, August 27, 2013, of *Proc Natl Acad Sci USA* (110:14456–14461; first published August 12, 2013; 10.1073/pnas.1307376110).

The authors note that Renée van Amerongen should be added to the author list between Taha A. Jan and Alan G. Cheng. Renée van Amerongen should be credited with having performed research and having contributed new reagents/analytic tools. The corrected author line, affiliation line, and author contributions appear below. The online version has been corrected.

Stefan Volkenstein[a,b], Kazuo Oshima[a,b], Saku T. Sinkkonen[a,b], C. Eduardo Corrales[a], Sam P. Most[a], Renjie Chai[a], Taha A. Jan[a], Renée van Amerongen[c], Alan G. Cheng[a], and Stefan Heller[a,b]

Departments of [a]Otolaryngology–Head and Neck Surgery and [b]Molecular and Cellular Physiology, Stanford University School of Medicine, Stanford, CA 94305; and [c]Division of Molecular Oncology, Netherlands Cancer Institute, 1066 CX, Amsterdam, The Netherlands

Author contributions: S.V., K.O., T.A.J., and S.H. designed research; S.V., K.O., S.T.S., C.E.C., S.P.M., R.C., T.A.J., and R.v.A. performed research; R.v.A. contributed new reagents/analytic tools; S.V., K.O., S.T.S., C.E.C., S.P.M., T.A.J., A.G.C., and S.H. analyzed data; and S.V., K.O., S.P.M., and S.H. wrote the paper.

www.pnas.org/cgi/doi/10.1073/pnas.1317787110

NEUROSCIENCE

Correction for "The role of long-range connections on the specificity of the macaque interareal cortical network," by Nikola T. Markov, Maria Ercsey-Ravasz, Camille Lamy, Ana Rita Ribeiro Gomes, Loïc Magrou, Pierre Misery, Pascale Giroud, Pascal Barone, Colette Dehay, Zoltán Toroczkai, Kenneth Knoblauch, David C. Van Essen, and Henry Kennedy, which appeared in issue 13, March 26, 2013, of *Proc Natl Acad Sci USA* (110:5187–5192; first published March 11, 2013; 10.1073/pnas.1218972110).

The authors note that Fig. 4 appeared incorrectly. The correct figure and its legend appear below.

Additionally, on page 5190, right column, first full paragraph, lines 21–22, "These values contrast with the interregion graph, in which the density is 50%" should instead appear as "These values contrast with the interregion graph, in which the density is 61%."

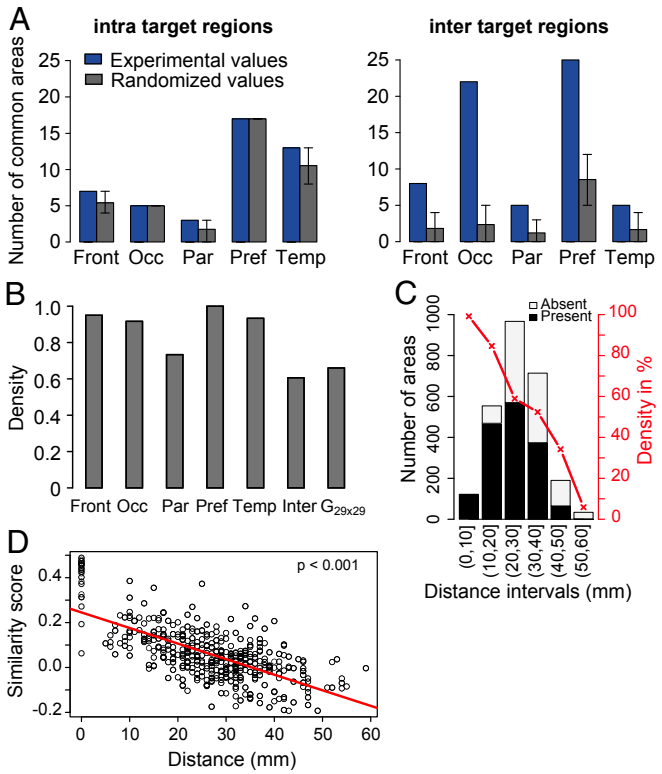

Fig. 4. Influence of distance on connectivity. (*A*) Number of intraregion (*Left*) and interregion (*Right*) common-source areas and effects of randomization of connections with preservation of target in-degree. Error bars, 5–95% quantiles after 2×10^4 permutation tests. (*B*) Density of the edge-complete graphs for intra- and interregions. (*C*) Histogram showing the number of connected and nonconnected areas at given distance intervals from injected target areas. Black bars, connected source areas; white bars, nonconnected areas. In red, connection density percentage (proportion of connected with respect to unconnected areas) of connectivity with distance. (*D*) Binary similarity index as a function of distance between target pairs. Abbreviations are the same as in Fig. 2.

www.pnas.org/cgi/doi/10.1073/pnas.1316840110

The role of long-range connections on the specificity of the macaque interareal cortical network

Nikola T. Markov[a,b,c], Maria Ercsey-Ravasz[d,e], Camille Lamy[a,b], Ana Rita Ribeiro Gomes[a,b], Loïc Magrou[a,b], Pierre Misery[a,b], Pascale Giroud[a,b], Pascal Barone[a,b,f], Colette Dehay[a,b], Zoltán Toroczkai[d], Kenneth Knoblauch[a,b,1], David C. Van Essen[g,1], and Henry Kennedy[a,b,2]

[a]Stem Cell and Brain Research Institute, Institut National de la Santé et de la Recherche Médicale U846, 69500 Bron, France; [b]Université de Lyon, Université Lyon 1, 69003 Lyon, France; [c]Department of Neurobiology, Yale University, New Haven, CT 06520; [d]Department of Physics, Interdisciplinary Center for Network Science and Applications, University of Notre Dame, Notre Dame, IN 46556; [e]Faculty of Physics, Babes-Bolyai University, 400084 Cluj-Napoca, Romania; [f]Cerveau et Cognition, Unité Mixte de Recherche 5549, 31059 Toulouse, France; and [g]Department of Anatomy and Neurobiology, Washington University School of Medicine, St. Louis, MO 63110

Edited by Jon H. Kaas, Vanderbilt University, Nashville, TN, and approved February 11, 2013 (received for review November 1, 2012)

We investigated the influence of interareal distance on connectivity patterns in a database obtained from the injection of retrograde tracers in 29 areas distributed over six regions (occipital, temporal, parietal, frontal, prefrontal, and limbic). One-third of the 1,615 pathways projecting to the 29 target areas were reported only recently and deemed new-found projections (NFPs). NFPs are predominantly long-range, low-weight connections. A minimum dominating set analysis (a graph theoretic measure) shows that NFPs play a major role in globalizing input to small groups of areas. Randomization tests show that (*i*) NFPs make important contributions to the specificity of the connectivity profile of individual cortical areas, and (*ii*) NFPs share key properties with known connections at the same distance. We developed a similarity index, which shows that intraregion similarity is high, whereas the interregion similarity declines with distance. For area pairs, there is a steep decline with distance in the similarity and probability of being connected. Nevertheless, the present findings reveal an unexpected binary specificity despite the high density (66%) of the cortical graph. This specificity is made possible because connections are largely concentrated over short distances. These findings emphasize the importance of long-distance connections in the connectivity profile of an area. We demonstrate that long-distance connections are particularly prevalent for prefrontal areas, where they may play a prominent role in large-scale communication and information integration.

monkey | anatomy | neocortex

The development of retrograde tract tracing methods has made possible high-resolution connectivity analysis in the central nervous system at the single-cell level (1). Considerable progress has been made in describing the functional regionalization of the cortex and the pathways linking cortical areas (2, 3). This progress has led to an understanding that the organization of interareal connections constrains the flow of information through the cortex. For instance, the constellation of cortical areas in different sensory modalities is interconnected by feedforward and feedback pathways forming hierarchical systems (4–6).

Improvements in tracer sensitivity and analysis methods have led to an increase in the number of identified interareal connections. In a recent study involving retrograde tracer injections into 29 cortical areas distributed reasonably evenly across the macaque cortex, each area was found to receive inputs from between 26 and 87 cortical areas in a cortical parcellation with 91 areas (7). Although many more experiments are needed to test all the pathways of the entire network of 91 areas ($\mathbf{G}_{91 \times 91}$), the earlier study provided an edge-complete cortical $\mathbf{G}_{29 \times 29}$ subgraph in which the connectivity status between any two nodes of the $\mathbf{G}_{29 \times 29}$ is fully known. Formally, a subgraph (in our case, $\mathbf{G}_{29 \times 29}$) of a graph ($\mathbf{G}_{91 \times 91}$) is edge complete if it has exactly the same connections between its nodes as the same nodes have in the larger graph. The $\mathbf{G}_{29 \times 29}$ subgraph has a density of 66% (i.e., 66% of the connections that may exist do exist). The study revealed a total of 1,615 pathways in the $\mathbf{G}_{29 \times 91}$ graph, more than one-third of which had not been reported previously in the literature and hence constitute new-found projections (NFPs) as opposed to the previously reported known projections (7). A dominating set analysis described the statistics of the global input to groups of areas revealed the existence of many small groups receiving connections from almost all other areas. In particular, there were two areas (8L and 7m) that together received input from all 91 areas, thus showing a minimum dominating set (MDS) of 2 for the $\mathbf{G}_{29 \times 91}$ graph (7).

Given the significantly high percentage of NFPs per source area (36%; range, 8–63%), here we investigat how these connections influence the statistical properties of cortical network organization. We show how the known projections and the NFPs of the 29 target areas are distributed across the major regions of the cortex. Our analysis reveals that the NFPs are predominantly long-distance connections constituting nearly half of all pathways between areas more than 20 mm apart. Thus, having missed the NFPs, previous studies underestimated the contributions of long-distance corticocortical connections, prompting us to investigate the effects of distance on connectivity and to capitalize on quantitative data that heretofore have been lacking. We report that long-distance connections in general (including the NFPs) make an important contribution to the specificity of interareal connectivity. This is surprising insofar as binary specificity (i.e., specificity that excludes consideration of connection weights) is unlikely a priori, given the overall high density of the cortical graph (7). Building on anatomical studies suggesting that cortical areas are connected to their neighbors more frequently than to more distant areas (8–12), we examined how distance influences the probability of being connected in the $\mathbf{G}_{29 \times 91}$ graph. Following earlier suggestions that physically nearby areas tend to have similar inputs and outputs (13, 14), we examined how distance influences the similarity of connectivity patterns in the $\mathbf{G}_{29 \times 91}$ graph. With increasing distance, there is a decline in the similarity and probability of being connected, the latter observation being a necessary condition for the observed high binary specificity of long-distance connections (both known projections and NFPs).

Author contributions: N.T.M., K.K., and H.K. designed research; N.T.M., M.E.-R., C.L., A.R.R.G., L.M., P.M., P.G., P.B., C.D., Z.T., and H.K. performed research; N.T.M., M.E.-R., C.L., A.R.R.G., L.M., P.M., P.G., P.B., C.D., Z.T., K.K., D.C.V.E., and H.K. analyzed data; and N.T.M., C.D., Z.T., K.K., D.C.V.E., and H.K. wrote the paper.

The authors declare no conflict of interest.

This article is a PNAS Direct Submission.

Freely available online through the PNAS open access option.

[1]K.K. and D.C.V.E. contributed equally to this work.

[2]To whom correspondence should be addressed. E-mail: henry.kennedy@inserm.fr.

This article contains supporting information online at www.pnas.org/lookup/suppl/doi:10.1073/pnas.1218972110/-/DCSupplemental.

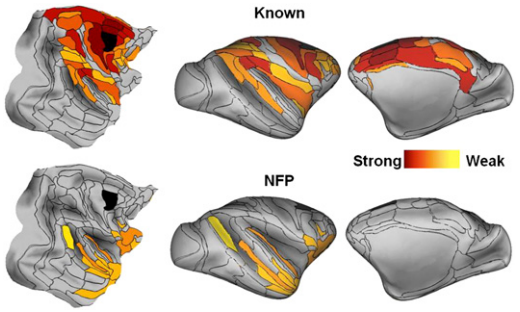

Fig. 1. Surface maps of cortical connectivity for an exemplar injected area (area F2, in black). (*Upper*) Known connections; (*Lower*) NFPs. (*Left*) Flat maps; (*Center*) lateral inflated maps; (*Right*) medial inflated maps. Connection strengths are color coded as values of $\log_{10}$(FLNe), varying from 0 (red) to −6 (yellow). Area injected is in black. See Fig. S1 for surface connectivity maps of the remaining 28 injected areas.

Results

Physical Layout of Source Areas with Respect to the Target Area. Fig. 1 shows an exemplar set of connectivity maps displayed on cortical surfaces (flat maps and lateral and medial inflated surfaces) for known projections and NFPs following an injection in F2 (see Fig. S1 for maps of the remaining 28 injections). Overall, the surface maps reveal that source areas form a group that covers between half and three-quarters of the cortical surface. The strongest connections (reddest hues) tend to be closest to the injection. Known connections form a more or less continuous territory surrounding the injected area. NFPs are rare in the immediate vicinity of the injected area but are common at intermediate and distant locations.

Regional Analysis of the Similarity of Connectivity. Fig. 1 and Fig. S1 show that strongly connected areas (known and NFP) tend to be grouped, suggesting that neighboring areas might share similar sets of connections (i.e., have similar connectivity profiles). To determine to what extent areas within each of the six cortical regions share similar connectivity profiles, we have defined a similarity index, which resembles the connectivity matching index developed in refs. 15 and 16 but has the advantage of taking into account both common connected and common nonconnected areas. More precisely, the similarity index measures the degree to which two areas receive input (or avoid receiving input) from common sources (in-link similarity) or project (or avoid projecting) to common target areas (see *SI Similarity Index* for definitions).

To assess the similarity of connectivity profiles for areas in the six different regions (occipital, temporal, frontal, parietal, prefrontal, and limbic), we computed the average similarity index of area pairs, for which one area is from region A and the other from region B. The out-link similarity between regions A and B then is obtained as the average similarity over all area pairs x (in A) and y (in B): $S^{out}_{AB} = \langle S^{out}_{xy} \rangle_{x\in A, y\in B}$ (Fig. 2*A*). A similar method is used to calculate the in-link similarity of the connectivity patterns of the 29 target areas across the six regions (Fig. 2*B*), $S^{in}_{AB} = \langle S^{in}_{xy} \rangle_{x\in A, y\in B}$. The diagonal for the similarity matrix represents the average similarity of the pairs of areas within each region. The limbic cortex has a row/column entry in the out-link similarity but not in the in-link similarity, because only a single limbic area was injected.

The pattern of similarity was consistent for in- and out-links, even though the incidence of nonreciprocal connections (~30%) was relatively high (7). High similarity values are concentrated along the positive diagonal (when $A = B$), and intraregion similarity is stronger than interregion similarity. For in-links, the highest intraregion similarity is in the occipital region and the lowest is in the temporal and parietal regions.

Interregion similarity tends to decrease with distance, but there are exceptions. For in-links, dissimilarity is greatest between the occipital (visual) and frontal (motor) regions; comparatively, the occipital and prefrontal regions show greater similarity, presumably because their areas have numerous long-distance connections (see below). Calculations of similarity based on a dot product between vectors of FLNe index (the fraction of labeled neurons in the source area with respect to the total number of labeled neurons extrinsic to the target area) for each region, yielding a cosine of the angle between the vectors, gave similar results (*SI Weighted Similarity* and Fig. S2).

Role of NFPs in Shaping the Global Input to Groups of Areas. Dominating set analysis is used in network theory to identify groups of areas that receive or provide the most direct influence with respect to the rest of the network. A subset of nodes D in a graph G is a dominating set if there is at least one connection from every node in the graph (including the set D) to a node in D. The MDS is defined as the dominating set with the smallest size (in the number of nodes). Elsewhere (7), we extended this definition to provide a more refined picture of the global input to groups of nodes in the cortex, by saying that D dominates x% of the nodes in G if x% of all the nodes in G are connected to at least one node in D. The case x% = 100%, i.e., when we have full domination, corresponds to the standard definition. We have shown (7) that the $MDS_{29\times 91} = 2$, which is very low and reflects the dense connectivity of the interareal network (Table S1); that is, there is a group of only two targets (8L, 7m) that receives input from all 91 areas. Because the inputs to an area do not change with increasing numbers of injections, this means (for the same parcellation) that additional data can only decrease the MDS, not increase it. Thus, for the full interareal network $G_{91\times 91}$ we must have $MDS_{91\times 91} \leq 2$. Additionally, 26.6%, or 108 of all two-area combinations of the 29 targets (there are 406 of them), will dominate 90–99% of all areas. There are 69 target triples (1.88%) that dominate the network fully. Similarly, there are 1,978 groups of four areas (8.33%) that fully dominate the network. Interestingly, all possible eight-target combinations (about 4.3 million) will dominate at least 90% of the whole network, as shown in Table S1. As we show next, the NFPs play a major role in the statistics of the inputs to area groups. Fig. S3 compares the statistics of the dominating sets between the network with all connections included (Fig. S3*A*) and the network based only on the known connections, that is, with the NFPs absent (Fig. S3*B*). The numerical values are shown in Tables S2 and S3.

Surprisingly, when the NFPs are excluded, the network does not have a fully dominating set (*SI Taking out NFP*). This is because there are two areas (subiculum and piriform) that have only NFP connections, and when NFPs are removed, these two areas become isolated (Table S2). We therefore repeated the dominating set analysis on 89 areas with these two isolated targets excluded. Even then, we see major differences in the dominating set statistics with

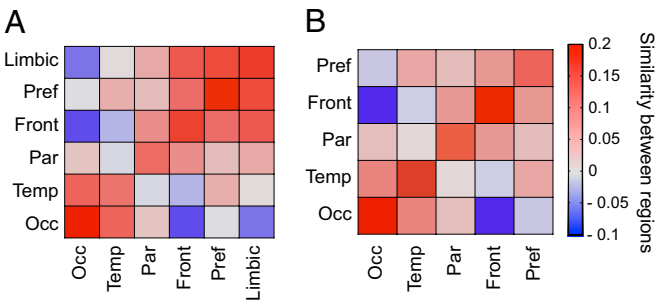

Fig. 2. Regional analysis of the similarity of binary connectivity patterns. Positive values indicate correlation; negative values indicate anticorrelation between the binary connectivity profiles of the pairs of areas located in cortical regions (color bar). (*A*) Out-link similarity. (*B*) In-link similarity. In both cases, the diagonal encodes the average intraregion similarity of area pairs, and the rest of the matrix the average interregion similarity of area pairs. Front, frontal region; Occ, occipital region; Par, parietal region; Pref, prefrontal region; Temp, temporal region.

and without NFPs. In particular, the MDS jumps from 2 to 5 and only 2.84% of all eight-target combinations fully dominate the network, whereas with the NFPs included, the same number is 65.96%, a 23-fold change. In general, full domination is reduced significantly for each of the group sizes (last vertical column in Fig. S3) with the NFPs absent. This suggests that as a contingent of long-distance connections, the NFPs have an important role in bringing global input to small, specific groups of areas and are part of a focused integration mechanism in cortical information processing. We tested this assertion further by also looking at the density of connections within the smallest groups with the largest domination. Information processing within the group would be indicated by strong connectivity (*SI Nodes with Strong Domination*). Indeed, as summarized in Table S4, the average density of connections within the fully dominating triplets is 85% whereas for quadruplets it is 73.6%, adding further evidence to the role of focused integration played by the NFPs.

Distance and Strength of NFPs. The NFPs to the areas in each cortical region constituted a substantial fraction of the total number of connections (limbic, 13%; prefrontal, 40%; frontal, 30%; parietal, 30%; temporal, 43%; and occipital, 37%). Fig. 3*A* shows a histogram of the number of known pathways (white bars) and of NFPs (red bars) in intervals of 0.5 $\log_{10}$(FLNe). On average, known connections are stronger than NFPs, but the FLNe values of the two populations overlap extensively. Indeed, a surprising 44% of the NFPs had FLNe of moderate strength ($-4 < \log_{10}(\text{FLNe}) < -2$), and a few (2%) are classified as strong connections ($-2 < \log_{10}(\text{FLNe}) < 0$). For very low FLNe values, NFPs correspond to at least 90% of the population but constitute a decreasing fraction of the source areas with increasing FLNe.

The proportion of NFPs increases with the estimated length of the 3D trajectory of pathways (Fig. 3*B*). Fig. 3*D* shows that the average trajectory of NFPs (27 ± 8.3 mm SD) is longer than for known projections (22 ± 9.5 mm SD; *t* test, $P < 0.001$). Although the overall ranges of the two types of projections were similar, NFPs were relatively rare at distances shorter than 17 mm, and compared with known projections, they more frequently link source and target areas in different regions (Fig. 3*E*). Within the injected region, only 11% of the projections are NFPs, compared with 37% outside the injected region (Fig. 3*E*).

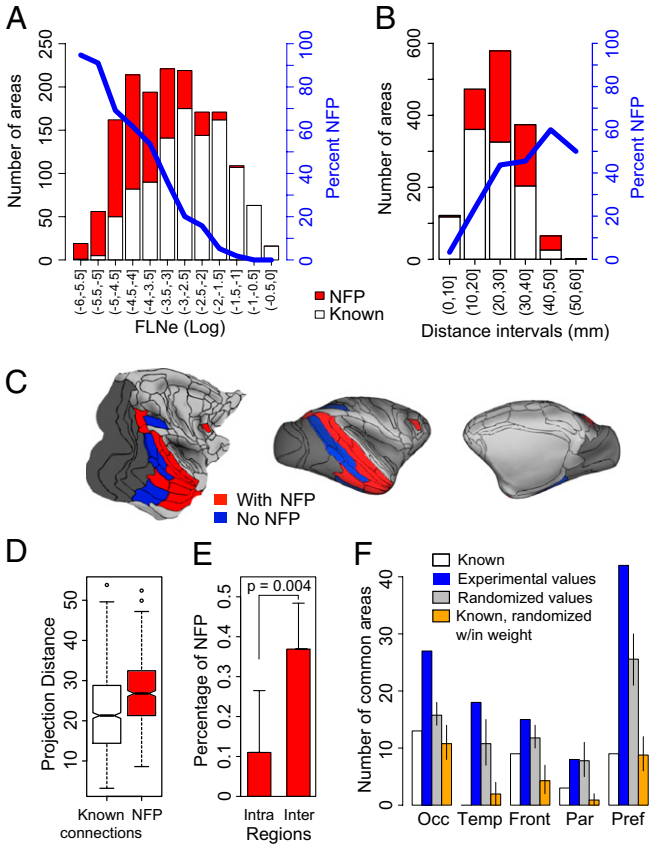

Fig. 3. Weight and distance characteristics of NFPs. (*A*) Distribution of known projections and NFPs as a function of projection strength (FLNe) at intervals of 0.5 $\log_{10}$(FLNe), generated after injection of the 29 target areas. Blue line, percentages of NFPs. (*B*) Influence of distance on proportions of known projections and NFPs. (*C*) Surface maps showing spatial relationships of the common-source area projections to target areas in the occipital region (shaded in dark gray). Areas projecting to all injected areas of a region via known connections are in blue and via known + NFPs in red. (*D*) Box plot analysis of projection distances of known projections and NFPs. (*E*) Intra- and interregion frequency of NFPs, one-sided *t* test; error bars represent SD. (*F*) Contribution of NFPs to regional connectivity signature. Numbers of common-source areas to target areas within a given region; see color code and text for details. Error bars in *F* indicate 95% confidence intervals. (*D* and *E*) Red bars, NFPs; white bars, known. Abbreviations are the same as in Fig. 2.

Regional Connectivity Signature and the Influence of NFPs. As we saw earlier, neighboring areas have similar connectivity profiles, so for two adjacent areas, there will be a relatively large number of other areas providing input to both. The shared inputs to the injected areas of a region represent a form of connectivity signature of that region. Because NFPs are predominantly long-distance connections from outside the region containing the target area, one surmises that the NFPs—or, more generally, the long-distance connections—play a special role in the connectivity signature of the injected areas in a region. Next, we investigate the role of NFPs in the connectivity signature of a region (*SI Common Source Signatures*).

Each of the five regions has a variable number of source areas providing common input. The influence of the NFPs on the common territory is evident on the inflated and flat map representations (Fig. 3*C* and Fig. S4), in which common source areas from long-distance connections are in blue and known + NFPs in red. In all cases, the inclusion of the NFPs markedly increased the number of cortical areas projecting to all the injected areas in a region (Fig. 3*F*, blue bars).

The injected areas in the occipital cortex (Fig. 3*C*) share inputs via known connections from 8 areas located in the temporal (TH/TF, TEpv, TEa/mp, TEOm, MT, FST, and V4t) and parietal (LIP) regions (see Table S5 for the complete nomenclature of the cortical areas). Inclusion of the NFPs greatly extends the number of common areas, adding 11 areas in the temporal region (dorsally up to areas MST and including the subdivisions of STPc, STPi, and STPr, and ventrally up to areas TEav and including the perirhinal area), 2 areas in the parietal region (areas PIP and DP), and 1 area in the prefrontal region (area 8L) (Fig. 3*C*).

Across the five regions from above, an average of 7% of the known inputs to each region are common sources to all the areas in a given region. The same percentage applied to known and NFPs combined increases to 19%. To address whether the effect of inclusion of NFPs on the increase in the number of common sources is a result of the specificity of the NFPs and not just the consequence of the increased density of connections, we carried out a permutation test in which NFPs were replaced by randomly selected projections drawn from the full set of areas that were not reported previously to project to the target area (Fig. 3*F*). In each cortical region except the parietal region, the number of common source areas observed significantly exceeds the mean number of common source areas in the randomly redistributed areas by a factor of 1.5 on average (median 1.6), and the 90% confidence intervals exclude the experimentally obtained values in every case except for the parietal region. The difference between the gray and white bars in Fig. 3*F* indicates the increase in common source areas to be expected solely on the basis of increased density.

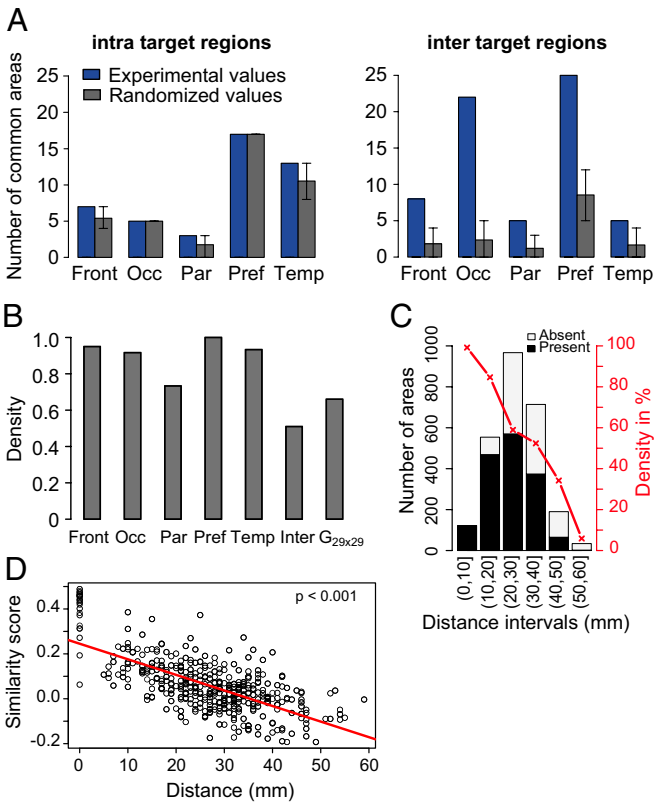

Fig. 4. Influence of distance on connectivity. (*A*) Number of intraregion (*Left*) and interregion (*Right*) common-source areas and effects of randomization of connections with preservation of target in-degree. Error bars, 5–95% quantiles after 2×10^4 permutation tests. (*B*) Density of the edge-complete graphs for intra- and interregions. (*C*) Histogram showing the number of connected and nonconnected areas at given distance intervals from injected target areas. Black bars, connected source areas; white bars, nonconnected areas. In red, connection density percentage (proportion of connected with respect to unconnected areas) of connectivity with distance. (*D*) Binary similarity index as a function of distance between target pairs. Abbreviations are the same as in Fig. 2.

Do the NFPs have a privileged role with respect to known connections in the common source signature? Fig. 3*F* tests this by a permutation analysis. For each target area, we have two categories: known and NFP. We permute connections across the two categories by randomly reassigning the labels of NFP and known within each density bin, as shown in Fig. 3*A*. This generates a set of connections that is numerically equal to the number of connections in the known category but is composed of randomly selected known connections and NFPs (orange bars). Comparison of orange and white bars in Fig. 3*F* shows similar numbers of common inputs. This observation is important because it suggests there is nothing special about the NFPs with respect to known connections in constraining the common input.

To summarize, the NFPs for each target area are not a random collection of additional connections, but instead constitute a distinct set of predominantly low-weight, long-distance connections. Their specificity is not different from that of known connections of the same distance. To understand why NFPs are so specific, we need to investigate the overall role distance plays in defining the cortical network. This we undertake in the next section.

Binary Specificity and Distance. Because of the high density of the $G_{29 \times 29}$ subgraph, one would expect little binary specificity. However, in Fig. 3*F* we saw that addition of NFPs caused a nearly threefold increase in common inputs and that randomization confirmed the specificity of the NFPs. Is the specificity related to their being long distance?

To examine this, we determined the incidence of common source areas for short distances (intraregion connections) and for long distances (interregion connections) and compared this with randomized patterns of connectivity (Fig. 4*A*). The extent to which the randomized values are lower than the experimentally observed values indicates the specificity of the connectivity. For sources and potential sources confined to the same region, observed and randomized values were very similar. By contrast, for interregion connectivity, the observed number of common sources to the sets of targets in each of the five regions (blue bars) was significantly higher than the average number occurring by the permutation analysis (gray bars). The results suggest there is little binary specificity of connections at short distances in the region in which the area is located, contrasting with the high degree of binary specificity for long-distance interregion connections. To examine this in more detail, we constructed the edge-complete intraregion subgraphs for the prefrontal, frontal, temporal, parietal, and occipital regions (gray bars in Fig. 4*B*) and the edge-complete interregion subgraph (interregion in Fig. 4*B*). The intraregion graph densities had a mean value of 90% (range, 70–100%). These values contrast with the interregion graph, in which the density is 50%. Compared with the intraregion networks, the low density of the interregion network allows for high specificity.

Injected areas receive projections from nearly all areas in their immediate vicinity; by visual inspection, the incidence of nonconnected areas increases with distance from the injected areas (Fig. 1 and Fig. S1). If this reflects differences in the density of connectivity with distance, it might explain the increase in binary specificity with distance shown in Fig. 4*A*. To investigate this possible effect of distance on connectivity, we quantified this relationship using an estimate of the within–white-matter distance between target areas and all other areas (both connected and not connected) (*Methods*). The percentage of source areas as a function of the total number of areas available at a given distance bin (Fig. 4*C*) showed a steady decline with distance. In the immediate vicinity of target areas, 99% of the areas present project to the target area. This declines to 85% at 10–20 mm, 50–60% at 20–40 mm, and below 40% beyond 40 mm.

The high connectivity density at short distances leaves little room for diversity at that scale, because nearly all areas are interconnected. This contrasts with the higher specificity and heterogeneity occurring for projections from areas separated by long distances. Because the similarity of connections is greater intraregionally compared with across regions (Fig. 2), we have examined whether there also is an effect of distance on the similarity of connections. Fig. 4*D* shows that neighboring targets have highly similar connectivity, which progressively decreases with separation between the target area pairs.

Regional Differences in Frequency of Long-Distance Connections. Previously, prefrontal areas were noted to receive many connections, i.e., to have a high in-degree (7). Here we show that compared with all other areas, the degree of the prefrontal areas is significantly higher (Fig. 5*A*). We then investigated whether the higher degree of the prefrontal cortex is associated with the areas in this region engaging in more long-distance connections compared with areas in other regions.

In Fig. 5*B*, the interregion connections were separated into two groups: those with either a prefrontal source or target and those excluding the prefrontal region as both source and target. The average difference in numbers of connections as a function of distance was calculated between the two groups (blue points). Prefrontal and nonprefrontal labels were permuted randomly, and the difference in the numbers of connections of the two groups as a function of distance was recomputed 10,000 times to yield a permutation distribution at each distance (17). We estimated the probability that the number of prefrontal connections at each distance is greater than or equal to the number of con-

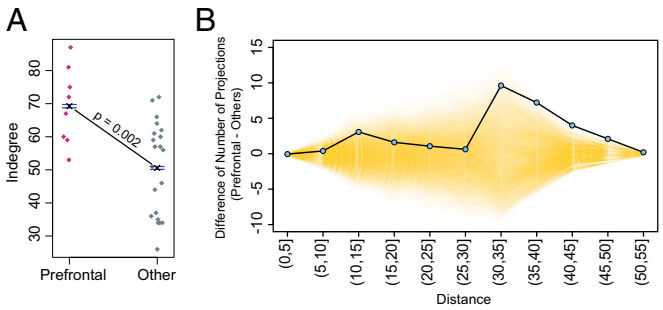

Fig. 5. Prefrontal cortex is characterized by a high in-degree distribution and long-distance interregion connectivity. (*A*) In-degree of prefrontal areas compared with all other regions. Dots indicate individual areas; one-sided *t* test with *P* value < 0.05. (*B*) Frequency of interregional connections in the prefrontal cortex, showing a preponderance of long-distance connections. Blue dots, difference between prefrontal long-distance connections and all other regions; yellow transparent lines, permuted values (for further details, see text).

nections involving all other regions. For a given distance, when the differences for permuted values (yellow in Fig. 5*B*) are less than the observed unpermuted data (blue points), then the prefrontal connections are significantly more numerous. All *P* values corrected for multiple testing were significant for distances greater than 40 mm, thus indicating that the prefrontal region participates in a greater number of long-range connections than all other regions combined (30–35 mm, $P = 0.01$; 35–40 mm, $P = 0.004$; 40–45 mm, $P < 0.001$; 45–50 mm, $P < 0.001$; and 50–55 mm, $P < 0.001$). Similar tests restricted to inputs to the prefrontal cortex (and thereby making sure the area dimensions in this region are not a confounding factor) give similar results.

The results of this study indicate that long-distance connections play a determinant role in the specificity of the cortical network. In this respect, it is of particular interest that the prefrontal cortex is characterized by a significantly greater number of long-distance connections compared with all other regions.

Discussion

NFPs and Known Connections. Long-distance connections play a special role in conferring specificity to the interareal network. There is a decrease in similarity and therefore an increase in dissimilarity with distance (Fig. 4*D*). This is because the majority of long-distance connections differentiate the connectivity profiles of neighboring target areas, in contrast to the minority (19%) that provide a common input to neighboring target areas, thereby defining the connectivity signature of the areas in a given region. We show that contrary to regional connections, long-distance connections exhibit a high degree of specificity and play an important role in determining the connectivity profiles of their targets. NFPs are a particular set of largely low-weight, long-distance connections. Our permutation analysis shows that the specificity of NFPs is similar to that of known connections at the same distances. The cortical graph is extremely dense (66%), so we would not expect there to be any binary specificity (7). However, we found that the probability of any two areas being connected declines with distance. In other words, in the $G_{29 \times 91}$, density is concentrated at short distances, thereby allowing the long-distance connections to be considerably sparser. Given the high average density, this sparser long-distance connectivity is the prerequisite for the high specificity that we observe in the long-distance connections and further underlines the importance of the NFPs.

Although the term "NFP" is potentially awkward, as the "newness" of these projections is of only relative value, we emphasize again that the connections of these pathways share similar statistical properties with those of known pathways at the same distance. Because the NFPs are predominantly long distance, our analysis shows they have an important impact on the specificity of interareal connectivity. The complete set of connections obtained by including the NFPs permits a more accurate analysis of the cortical network.

Role of Distance on Cortical Organization. The cerebral cortex exhibits local structural and functional continuity in ways that also respect the distinctness of adjoining areas (18–20). This may contribute to clustering of functionally related areas and minimization of aggregate wiring (21–24). A corollary prediction is that interareal connectivity should be influenced by distance. Indeed, we found that connectivity similarity changes as a smooth function of distance (Fig. 4*D*), which echoes other gradual changes across the cortex, such as the size of dendritic arbors (25), the extent of intrinsic connectivity (26), and gene expression (27).

The factors influencing the frequency of common source areas illustrate how specificity of connectivity is determined. The common-source, long-distance connections constitute a connectivity signature for a set of areas in a particular locality. Given that only a selection of the areas in a region have been investigated, the set of common inputs will evolve as the number of areas injected increases, so further injections will be necessary to determine the full repertoire of common-source areas. In the present results, the two regions most strikingly influenced by shared common input are the occipital and prefrontal regions (Fig. 3*C* and Fig. S4).

Area 7m, like 8L, has a very large in-degree that fits with the extensive connectivity of the precuneus region, as reported in both human and monkey (28, 29).

Shared inputs to the occipital cortex stretch from the ventral parietal cortex through most of the temporal cortex, plus the frontal eye field area (areas 8L and 8m) in the prefrontal cortex. The extensive common input from the temporal to the occipital region is consistent with the physiological importance of feedback to early visual areas (30). The finding that area 8L projects consistently to occipital areas points to the widespread role of eye movements in the physiology of early visual processing (31). Interestingly, the second component of the frontal eye field, area 8m, provides a widespread input to the parietal cortex (all areas barring areas 5 and 2). These differences concerning the relationship of the frontal eye field with the parietal and occipital cortices are consistent with distinct requirements for the processing of large (area 8m) and small saccades (area 8L) (32).

Shared input to the prefrontal cortex originates from extensive portions of the frontal and limbic cortex plus the temporal and parietal cortex. Interestingly, the extensive territory sending common input to the prefrontal region largely is not reciprocated, similar to the situation for the occipital cortex.

Conclusion. The present findings show that long-distance connections make important contributions to the specificity of the cortical network. Weights of the pathways linking cortical areas show a high heterogeneity spanning five to six orders of magnitude, suggesting that weight plays an important role in specifying the physiological function of a cortical area (7). Although long-distance connections overall are weak, they nevertheless are highly consistent across brains (7, 13), and one can hypothesize that their primary role is in communication via coordinating oscillatory activity (33). Long-distance connections in the occipital cortex have been proposed to play a prominent role in imagery and multisensory integration (34). The global neuronal workspace model of consciousness predicts the long-distance connections that we show characterize the prefrontal cortex and that have been hypothesized to ignite large-scale cortical networks (35, 36).

The present findings explore the large contingent of long-distance connections, which were not detected previously. The $\mathbf{G}_{29 \times 91}$ shows a high density (7). Because of the decreasing probability of connectivity with distance, the $\mathbf{G}_{29 \times 91}$ subgraph exhibits an unsuspected high-degree of binary specificity of long-distance connections. This underlines the importance of the NFPs, because they are a major contingent of the long-distance connections. Additionally, as part of the long-distance connectivity,

the NFPs play an important role in the globalization of input to small groups of areas, thereby contributing to the focused integration mechanism provided by the core structure suggested in earlier studies using "rich-club"–type network measures (expressing the extent to which central nodes have more interconnections than expected at random) (37).

Future investigations are required to uncover the long-distance connections (equivalent to the NFPs here) we confidently assume remain to be discovered in the 62 areas we have not injected here; presumably, the NFPs were missed in earlier studies because they tended to focus on connectivity in the vicinity of the injected area (7). Because of the low weight of long-distance connections, this work cannot be carried out by existing imaging techniques but instead require the gold standard provided by quantitative tract tracing (7, 13, 38, 39). As shown here, these long-distance connections are important in characterizing the connectivity of regions and the individuality of the connectivity profiles of areas. It remains to be seen whether long-distance connections exhibit unique properties, such as synaptic morphologies (40) or molecular identities of the parent neurons (27, 41, 42). Overall, the present results point to the need to fully embrace the large-scale connectivity of the cortex if we are to resolve how its overall structural complexity relates to its function.

Methods

Surgical and histology procedures were in accordance with European requirements 86/609/EEC and approved by the ethics committe of the region Rhône-Alpes.

Connectivity Data. We used the retrograde tracing connectivity data reported in Markov et al. (7). The injected area is referred to as the target area and the area containing labeled neurons as the source area. The 29 target areas are V1, V2, V4, TEO, 9/46d, F5, 8m, 7A, DP, 2, 5, 7B, STPr, STPi, STPc, PBr, TEpd, 24c, FI, F2, F7, ProM, 8L, 9/46v, 46d, 8B, MT, 7m, and 10. The weights of the projections were defined by their FLNe index, which is defined as the fraction of labeled neurons located in the source area with respect to the total number of labeled neurons extrinsic to the target area. Detailed descriptions of injection sites, FLNe values, and the parcellation of the cortical areas may be found in ref. 7. (Updates, atlases, and additional information are available at www.core-nets.org). Distances between areas were determined by minimum white matter trajectories (*SI Methods*).

Influence of Locality on Connectivity. To investigate the shared characteristics of the long-distance connectivity of neighboring areas, we defined six regions (Table S5). Three of these regions correspond to the parietal, temporal, and occipital cortical lobes. We subdivided the frontal lobe into frontal and prefrontal regions. Midline areas surrounding the corpus callosum were combined into a limbic region. For a more global assessment of the regions, see Fig. 3*C* and Fig. S4.

ACKNOWLEDGMENTS. We thank Michael Pfeiffer for insightful and critical reading of the manuscript; B. Beneyton, F. Piolat, M. Seon, and M. Valdebenito, for animal husbandry; E. Reid for cortical surface reconstruction; V. Vezoli for administrative assistance; and D. Dierker and J. Harwell for software development. This work was supported by FP6-2005 IST-1583, ANR-05-NEUR-088, ANR-11-BSV4-501, Region Rhône-Alpes Cible 2011, and LabEx CORTEX (H.K.); National Institutes of Health Grant R01-MH-60974 (D.C.V.E.); HDTRA-1-09-1-0039 and National Science Foundation Grant BCS-0826958 (Z.T. and M.E.-R.); and FP7-PEOPLE-2011-IIF-299915 (M.E.-R.).

1. Lanciego JL, Wouterlood FG (2011) A half century of experimental neuroanatomical tracing. *J Chem Neuroanat* 42(3):157–183.
2. Bressler SL, Menon V (2010) Large-scale brain networks in cognition: Emerging methods and principles. *Trends Cogn Sci* 14(6):277–290.
3. Rosa MG, Tweedale R (2005) Brain maps, great and small: Lessons from comparative studies of primate visual cortical organization. *Philos Trans R Soc Lond B Biol Sci* 360(1456):665–691.
4. Felleman DJ, Van Essen DC (1991) Distributed hierarchical processing in the primate cerebral cortex. *Cereb Cortex* 1(1):1–47.
5. Rockland KS, Pandya DN (1979) Laminar origins and terminations of cortical connections of the occipital lobe in the rhesus monkey. *Brain Res* 179(1):3–20.
6. Markov NT, Kennedy H (2013) The importance of being hierarchical. *Curr Opin Neurobiol* 23, 10.1016/j.conb.2012.1012.1008.
7. Markov NT, et al. (2013) A weighted and directed interareal connectivity matrix for macaque cerebral cortex. *Cereb Cortex*, 10.1093/cercor/bhs1270.
8. Burman KJ, Reser DH, Yu HH, Rosa MG (2011) Cortical input to the frontal pole of the marmoset monkey. *Cereb Cortex* 21(8):1712–1737.
9. Lewis JW, Van Essen DC (2000) Corticocortical connections of visual, sensorimotor, and multimodal processing areas in the parietal lobe of the macaque monkey. *J Comp Neurol* 428(1):112–137.
10. Lyon DC, Kaas JH (2002) Evidence for a modified V3 with dorsal and ventral halves in macaque monkeys. *Neuron* 33(3):453–461.
11. Wang Q, Burkhalter A (2007) Area map of mouse visual cortex. *J Comp Neurol* 502(3): 339–357.
12. Young MP (2002) Connectional organisation and function in the macaque cerebral cortex. *Cortical Areas: Unity and Diversity*, eds Schuz A, Miller R (Taylor and Francis, London), pp 351–376.
13. Markov NT, et al. (2011) Weight consistency specifies regularities of macaque cortical networks. *Cereb Cortex* 21(6):1254–1272.
14. Young MP, et al. (1995) Non-metric multidimensional scaling in the analysis of neuroanatomical connection data and the organization of the primate cortical visual system. *Philos Trans R Soc Lond B Biol Sci* 348(1325):281–308.
15. Sporns O (2002) *Graph Theory Methods for the Analysis of Neural Connectivity Patterns. Neuroscience Databases* (Kluwer, Dordrecht), pp 169–183.
16. Kaiser M, Hilgetag CC (2004) Edge vulnerability in neural and metabolic networks. *Biol Cybern* 90(5):311–317.
17. Efron B, Tibshirani RJ (1993) *An Introduction to the Bootstrap* (Chapman and Hall, New York).
18. Aflalo TN, Graziano MS (2011) Organization of the macaque extrastriate visual cortex re-examined using the principle of spatial continuity of function. *J Neurophysiol* 105(1):305–320.
19. Graziano MS, Aflalo TN (2007) Mapping behavioral repertoire onto the cortex. *Neuron* 56(2):239–251.
20. Douglas RJ, Martin KA (2012) Behavioral architecture of the cortical sheet. *Curr Biol* 22(24):R1033–R1038.
21. Cherniak C (1994) Component placement optimization in the brain. *J Neurosci* 14(4): 2418–2427.
22. Kaas J (2000) Why is brain size so important: Design problems and solutions as neocortex gets bigger or smaller. *Brain Mind* 1(1):7–23.
23. Klyachko VA, Stevens CF (2003) Connectivity optimization and the positioning of cortical areas. *Proc Natl Acad Sci USA* 100(13):7937–7941.
24. Van Essen DC (1997) A tension-based theory of morphogenesis and compact wiring in the central nervous system. *Nature* 385(6614):313–318.
25. Elston GN, Tweedale R, Rosa MG (1999) Cortical integration in the visual system of the macaque monkey: Large-scale morphological differences in the pyramidal neurons in the occipital, parietal and temporal lobes. *Proc Biol Sci* 266(1426):1367–1374.
26. Lund JS, Yoshioka T, Levitt JB (1993) Comparison of intrinsic connectivity in different areas of macaque monkey cerebral cortex. *Cereb Cortex* 3(2):148–162.
27. Yamamori T (2011) Selective gene expression in regions of primate neocortex: implications for cortical specialization. *Prog Neurobiol* 94(3):201–222.
28. Margulies DS, et al. (2009) Precuneus shares intrinsic functional architecture in humans and monkeys. *Proc Natl Acad Sci USA* 106(47):20069–20074.
29. Hagmann P, et al. (2008) Mapping the structural core of human cerebral cortex. *PLoS Biol* 6(7):e159.
30. Lamme VA, Roelfsema PR (2000) The distinct modes of vision offered by feedforward and recurrent processing. *Trends Neurosci* 23(11):571–579.
31. Ekstrom LB, Roelfsema PR, Arsenault JT, Bonmassar G, Vanduffel W (2008) Bottom-up dependent gating of frontal signals in early visual cortex. *Science* 321(5887):414–417.
32. Schall JD, Morel A, King DJ, Bullier J (1995) Topography of visual cortex connections with frontal eye field in macaque: Convergence and segregation of processing streams. *J Neurosci* 15(6):4464–4487.
33. Fries P (2005) A mechanism for cognitive dynamics: Neuronal communication through neuronal coherence. *Trends Cogn Sci* 9(10):474–480.
34. Clavagnier S, Falchier A, Kennedy H (2004) Long-distance feedback projections to area V1: Implications for multisensory integration, spatial awareness, and visual consciousness. *Cogn Affect Behav Neurosci* 4(2):117–126.
35. Harriger L, van den Heuvel MP, Sporns O (2012) Rich club organization of macaque cerebral cortex and its role in network communication. *PLoS ONE* 7(9):e46497.
36. Dehaene S, Changeux JP (2011) Experimental and theoretical approaches to conscious processing. *Neuron* 70(2):200–227.
37. van den Heuvel MP, Kahn RS, Goñi J, Sporns O (2012) High-cost, high-capacity backbone for global brain communication. *Proc Natl Acad Sci USA* 109(28):11372–11377.
38. Bakker R, Wachtler T, Diesmann M (2012) CoCoMac 2.0 and the future of tract-tracing databases. *Front Neuroinform* 6:6.
39. Sporns O (2011) *Networks of the Brain* (MIT Press, Cambridge, MA).
40. Anderson JC, Binzegger T, Martin KA, Rockland KS (1998) The connection from cortical area V1 to V5: A light and electron microscopic study. *J Neurosci* 18(24):10525–10540.
41. Hof PR, Nimchinsky EA, Morrison JH (1995) Neurochemical phenotype of corticocortical connections in the macaque monkey: Quantitative analysis of a subset of neurofilament protein-immunoreactive projection neurons in frontal, parietal, temporal, and cingulate cortices. *J Comp Neurol* 362(1):109–133.
42. Bernard A, et al. (2012) Transcriptional architecture of the primate neocortex. *Neuron* 73(6):1083–1099.